

Rapid in situ photochemical synthesis of carbon dots in polymer coating by infrared CO₂ laser writing for color tunable fluorescent patterning

Guo, Yuanyuan; Gao, Yixun; Wang, Yao; Lee, Yi Kuen; French, Patrick J.; Umar Siddiqui, Ahmad M.; Li, Hao; Zhou, Guofu

DOI

10.1016/j.cej.2024.158749

Publication date 2025

Document VersionFinal published version

Published in Chemical Engineering Journal

Citation (APA)

Guo, Y., Gao, Y., Wang, Y., Lee, Y. K., French, P. J., Umar Siddiqui, A. M., Li, H., & Zhou, G. (2025). Rapid in situ photochemical synthesis of carbon dots in polymer coating by infrared CO_laser writing for color tunable fluorescent patterning. *Chemical Engineering Journal*, *504*, Article 158749. https://doi.org/10.1016/j.cej.2024.158749

Important note

To cite this publication, please use the final published version (if applicable). Please check the document version above.

Copyright

Other than for strictly personal use, it is not permitted to download, forward or distribute the text or part of it, without the consent of the author(s) and/or copyright holder(s), unless the work is under an open content license such as Creative Commons.

Takedown policy

Please contact us and provide details if you believe this document breaches copyrights. We will remove access to the work immediately and investigate your claim.

Green Open Access added to TU Delft Institutional Repository 'You share, we take care!' - Taverne project

https://www.openaccess.nl/en/you-share-we-take-care

Otherwise as indicated in the copyright section: the publisher is the copyright holder of this work and the author uses the Dutch legislation to make this work public.

\$ SUPER

Contents lists available at ScienceDirect

Chemical Engineering Journal

journal homepage: www.elsevier.com/locate/cej



Rapid *in situ* photochemical synthesis of carbon dots in polymer coating by infrared CO₂ laser writing for color tunable fluorescent patterning

Yuanyuan Guo ^a, Yixun Gao ^a, Yao Wang ^{a,*}, Yi-Kuen Lee ^b, Patrick J. French ^c, Ahmad M. Umar Siddiqui ^d, Hao Li ^a, Guofu Zhou ^a

ARTICLE INFO

Keywords: Carbon dots Colorful fluorescent pattern CO₂ laser writing In situ photothermal reaction Anti-counterfeiting

ABSTRACT

The significant *in situ* multicolored patterning without changing printing tools nor substrate media still remains challenging, especially toward practical applications for anti-counterfeiting. This research invented a unique universal approach for the laser-induced *in situ* synthesis of colorful fluorescent patterns (from blue: CIE 0.15, 0.18 to red orange: CIE 0.36, 0.39) through the controlled formation of N, S doped carbon dots (CDs) in solid composite polymer films or hydrogel with a hierarchical and physically unclonable microsurface architecture for anti-counterfeiting. The *in situ* patterning approach, coupled with multi-layer technique, yielding designable blue, yellow, orange, and red orange color under 365 nm in the same pattern. A 5 cm² colorful pattern can be efficiently finished within 5 min without changing the substrate and the line width accuracy can be up to 300 μ m. The absolute quantum efficiency of the blue pattern reached as high as 23%. The fluorescent patterns can be survived at indoor for 24 months. The hydrogen bonding interactions between the CDs precursor and polymer facilitated the generation, uniform dispersion and stabilization of CDs during the laser irradiation. The hypothesis that laser irradiation induced photochemical reactions of CD precursors within a polymer matrix was supported by thermodynamic assessments. The universality of *in situ* fluorescent patterning strategy was demonstrated by developing fluorescent patterns on both solid polymer films, hydrogel, pharmaceutical packaging and textile.

1. Introduction

From indoor to outdoor environments, and across scales from micro to macro dimensions, colorful photoluminescence patterns have extensive applications, including displays, sensors, anti-counterfeiting, and signage [1–6]. Especially, for applications like fluorescent anti-counterfeiting and information encryption, the incorporation of full color fluorescent patterns could enhance the security level. Consequently, there exists a necessity to devise a technique of facilitating the creation of comprehensive full color fluorescent patterns. The generation of colorful fluorescent patterns can be accomplished using techniques such as inkjet printing, overlay printing-based silkscreen

methods, and multi-step lithography. For inkjet printing, achieving uniform luminescence in the resulting patterns necessitates the development of suitable fluorescent ink formulations. Additionally, technical challenges, such as mitigating inhomogeneous defects caused by the coffee ring effect, must be addressed to ensure consistent performance [7]. Ideally, for practical applications, achieving colorful fluorescent patterns on one piece of continuous film based on non-toxic materials and employing a straightforward fabrication method would be advantageous. However, it posed a straitened circumstance to reaching both of the above criteria simultaneously, given the intricate nature of the materials and processes involved in luminescent pattern formation.

Carbon Dots (CDs), as a novel class of fluorescent materials, offer

E-mail address: wangyao@m.scnu.edu.cn (Y. Wang).

^a Guangdong Provincial Key Laboratory of Optical Information Materials, Technology & Institute of Electronic Paper Displays and National Center for International Research on Green Optoelectronics, South China Academy of Advanced Optoelectronics, South China Normal University, Guangzhou 510006, PR China

b Department of Mechanical & Aerospace Engineering, Department of Electronic & Computer Engineering, Hong Kong University of Science and Technology, Clear Water Bay, Kowloon, Hong Kong Special Administrative Region

c EEMCS, Delft University of Technology, 2628 CD Delft, the Netherlands

d Department of Chemistry, Faculty of Science and Arts and Promising Centre for Sensors and Electronic Devices (PCSED), Najran University, Najran 11001, Saudi Arabia

 $^{^{\}ast}$ Corresponding author.

distinct advantages, including low toxicity, tunable optical properties, and notable photostability [8,9]. Due to their extremely small size and abundance of surface defects, CDs produce fluorescence at specific wavelengths by electrons jumping between energy levels when excited by external energy. At the same time, the quantum confinement effect restricts the movement of electrons within the CDs, while the surface defects provide additional energy levels, facilitating the excitation and leapfrog process. The manipulation of precursor selection and synthesis conditions allows for the alteration of functional groups on both the surface and core of CDs, yielding full fluorescent color CDs [10,11]. The straightforward fabrication of a single-color fluorescent polymer film was achievable by simply blending an appropriate concentration of CDs or CDs precursors into the polymer matrix [12,13]. The dispersion or formation of CDs occurred in the liquid phase within the polymer matrix during the process of heating and drying to form composite film. The interactions between CDs surface functional groups and polymer chains effectively eliminated fluorescence quenching due to aggregation and inhibit non-radiative transition, thereby enabling the production of solid-state fluorescent polymer films [14-19]. High resolution, large area multicolor fluorescent pattern can be effectively obtained by inkjet printing, yet the process limits material selectivity due to the ink surface tension, viscosity and solvent orthogonality of adjacent layers. To achieve multicolor fluorescent in a single pattern, different colored CDs inks must be formulated to meet the specifications for inkjet printing [20]. Besides inkjet printing, fluorescent patterns could be fabricated by laser pyrolysis or laser-assisted deposition[21-24]. Laser pyrolysis is one of the CDs synthesis methods, that exhibits the capability of thermal decomposition and inducing photoreaction between small molecules [25–27]. The thermal effect during laser writing is required for carbonation during the CDs generation process. The intrinsic bandgap emission of the sp²-conjugated domains in carbon core of CDs was considered responsible for the luminescence [28,29]. It is generally acknowledged that, laser-assisted CDs preparation represented one of the top-down synthesis methods, primarily driven by the thermal decomposition of larger molecular[30].

In 2023, through the integration of the CDs synthesis methodology with laser writing technologies, our prior research innovatively demonstrated the feasibility of in situ generating CD-based monochromatic fluorescent patterns via laser direct writing on a cellulose acetate butyrate film in air [31]. Recently, Zhang et al. reported that different CD-based color fluorescent patterns were achieved utilizing a laser-assisted nano-printing technique [32]. However, to the best of our knowledge, multicolor fluorescent pattern on one piece of monolithic polymer film has not been managed so far, since different CDs precursor contained film on the intermediate layer have to be switched for different colors. As we know, in addition to thermal decomposition, the intense infrared (IR) photons emitted by pulsed CO2 lasers can facilitate reactions between two reactants by transferring photon energy, thereby accelerating them into an excited state [25]. Thus the formation process of CDs is dependent with variation of pulsed CO2 lasers energy. Therefore, it is reasonable to assume that different color fluorescent CDs in polymer films would be generated by IR CO2 laser-induced in situ photochemical reactions which can be regulated through laser scanning rate control. Unlike the reported IR laser-induced organic reactions in high-pressure gas phases, solid-phase reactions induced by IR laser radiation under mild conditions scarcely reported.

In this work, a one-step generation of CD-based multicolor fluorescent pattern was developed via a laser-induced photochemical reaction in air. This achievement combined *in situ* CDs formation within a solid polymer film with construction of multilayer membrane structures. The fluorescent color can be modulated by adjusting the laser scanning rate even on a single polymer film. To verify the versatility of our approach, a hydrogel made from the same material system was also employed. The resulting multicolor fluorescent patterns exhibit distinct optical performance and a physically unclonable surface structure.

2. Experimental Section

2.1. Multilayer polymer substrate preparation

A 20 wt% Polyvinyl Alcohol (PVA) solution was formulated by dissolving PVA (1788, Sigma) in hot water at 90°C. For the yellow and orange fluorescence pattern, precursors of citric acid and thiourea (99%, Merck) were incorporated into the PVA solution (solution 1). In parallel, for the creation of a blue fluorescence pattern, a precursor of citric acid (anhydrous, 99.5%, Merck) and urea (99%, Merck) were introduced into the PVA solution (solution 2). Varied molar ratios of citric acid: urea and citric acid: thiourea, along with diverse total weight concentrations were used, as detailed in Table S1.

A 10 wt% and 20 wt% solution of cellulose acetate butyrate (CAB, 35–39 %, Aladdin) was prepared in ethyl acetate. For the double-layer structure, 20 wt% CAB was coated under solution 1 or 2. To construct a multilayer polymer film, the following sequence of layers was spin-coated onto glass substrates: 20 wt% CAB, citric acid/thiourea PVA solution (solution 1), 10 wt% CAB solution, and citric acid/urea PVA solution (solution 2). Each layer underwent room-temperature drying after spin coating. In addition, hydrogels based on solution 1 and solution 2 were fabricated using the freeze-dry method [33]. The solutions of 1 and 2 were applied to the surfaces of thoroughly cleaned tablet packages and fabrics using dip-coating and blade-coating techniques, respectively. Following natural drying, the QD code and SCNU school bandage were inscribed onto the coated surfaces using laser writing.

2.2. Colorful fluorescent patterning by laser writing

A CO $_2$ laser machine, specifically sourced from Shang Hai AoJian Laser Co., Ltd, was employed for the precision drawing of fluorescence patterns onto the polymer film in an ambient air environment. The wavelength of the CO $_2$ plus laser was 10.6 μ m with a rated power of 40 W. For all laser writing processes 15 % of rated power, 25 kHz frequency, and 0.02 mm line space were selected. Different colors of fluorescent patterns can be obtained by varying the scan rate. The patterns were designed by the laser machine drawing software.

2.3. Material and fluorescent patterns characterization

The thermal characteristics of solution 1 and solution 2 were analysed using thermogravimetric analysis (TGA, METTLER). The glass transition temperature (Tg) was determined by METTLER TOLEDO differential scanning calorimetry with a heating rate of 10 $^{\circ}$ C/min. To gain insights into the activation energy of the composite polymer film originating from solution 1 and solution 2, the Ozawa-Flynn-Wall method was employed. This method, aligned with the ISO11358-2:2014(E) standard, facilitated the determination of the activation energy, offering valuable information about the thermochemical behaviour of the polymer films.

Following the laser-writing procedure on the polymer films, the CDs were extracted through the dissolution of the laser-patterned film in cold water over three days. The resultant solution underwent concentration, followed by a seven-day dialysis process with a molecular weight cut-off (MWCO) of 1000 kDa. Subsequently, CDs solutions were obtained after further concentration and centrifugation at 10000 rpm for 10 min. The optical properties of the CDs solutions were examined utilizing a luminescence spectrometer (RF-6000, Shimadzu, Japan) and a UV-vis spectrophotometer (UV-1750, Shimadzu, Japan). The morphology of the CDs was characterized through Transmission Electron Microscopy (TEM) using a JEM-2010 instrument from JEOL, Japan. Additionally, Xray Photoelectron Spectroscopy (XPS) conducted on a Thermo Fisher Scientific apparatus equipped with an Al source (h $\nu=1468.6$ eV) was employed to analyse the elemental composition of the CDs. XRD (BRUKER D8 ADVANCE DAVINCI) was used to analyze the graphitization of the CDs. The Fourier-transform infrared spectrometer (Nicolet 6700) was utilized to analyse composition changes post-laser writing. The infrared spectroscopy and variable temperature infrared spectroscopy are analysed with Bruker Vertex 70, Germany. Furthermore, the quantum yield of the fluorescence patterns at 365 nm was measured by an absolute PL quantum yield spectrometer C11347 series (HAMA-MATSU). The surface temperature during the laser direct writing process was monitored using a FLIR A 6700 mid-wave infrared thermal imager, and the surface topography of the patterned areas was quantified using a DECTEC 3D profiler.

3. Results and discussion

3.1. Multicolor fluorescent patterns draw by CO₂ laser

Laser writing serves as a versatile technique for modifying the physicochemical attributes of transparent polymer films [34]. The hydrothermal reaction involving citric acid, urea, or thiourea is a classical method for CDs synthesis. The variation of fluorescent properties in CDs solutions were achieved by adjusting the proportions of citric acid and urea, alongside modifications in reaction conditions. In general, the type and quantity of surface-doping elements and the size of CDs commonly influenced the resultant fluorescent color diversity in CDs synthesis. Similarly, by introducing citric acid/urea or citric acid/thiourea into a PVA solution, multilayer composite polymer film with uniform-thickness can be successfully fabricated through spin coating onto a glass substrate. After employing laser writing (4 W, 25 kHz), fluorescence patterns can be deftly produced *in situ* on the surfaces of double-layer and multilayer films (Fig. 1).

The fluorescence created from the double-layer structure was initially investigated (Fig. 2). A $7.0 \, \mu m$ CAB film was applied beneath the

PVA composite polymer film as the base layer and peelable layer. The total thickness of double was 40 \pm 2 $\mu m.$ The film from PVA solution1 (PVA1) demonstrated transparency within the visible light spectrum (90 % transmittance), while at 10.6 μ m, a transmittance of 80 % was observed, which meant the CO₂ laser can be absorbed (Fig. S1a). During laser writing process, the absorption of the CO2 laser was expected to intensify due to alterations in surface structure and components. The upper layer of PVA1 underwent complete pyrolysis and gasification at scanning rates between 1000 and 1800 mm/s. Below 1000 mm/s, the laser writing etched on the CAB layer, resulting in the formation of CDs within the CAB film (Fig. 2a) [31]. The resulting CDs-composited CAB patterns displayed a light yellow-green fluorescence, suggesting that the CAB layer and the PVA1 film did not merge during laser writing at speeds below 1000 mm/s. As depicted in Fig. 2f, the solid-state fluorescence exhibited excitation dependence consistent with the characteristic luminescence features of CDs. The modulation of the scan rate within the range of $2000 \sim 3500$ mm/s yielded a transition in fluorescence color from yellow (CIE 0.34,0.36) to orange (CIE 0.36,0.39), with maximum fluorescence intensity achieved at 2200 mm/s and 3500 mm/ s, respectively (Fig. 2f). The surface roughness increased while the etch depth decreased with rising scan rate due to less accumulated adsorbed energy (Fig. \$2,3). At scan rates exceeding 1800 mm/s, laser writing predominantly affected the PVA1 layer, leading to the formation of bubble-like morphologies and an increase in film thickness. For comparison, laser writing was also conducted on a single-layer PVA1 film, varying the scan rate from 1000 mm/s to 3500 mm/s. The resulting fluorescent patterns all exhibited yellow color without any gradual changes, revealing that the CAB layer would influence the color variation (Fig. S4a). The line widths by laser writing range from 320 to 1100 μm at the same laser scanning rate (Fig. S4c). The IR photon-induced

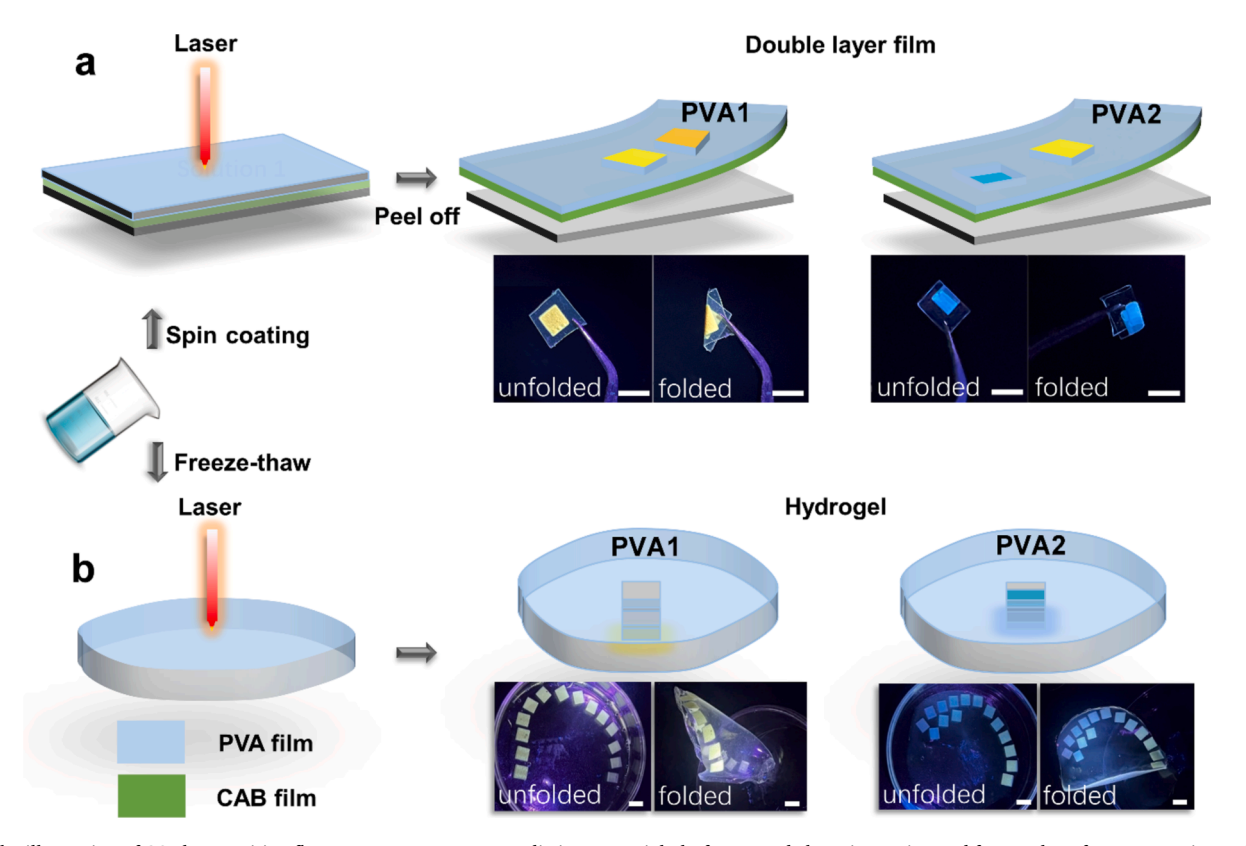
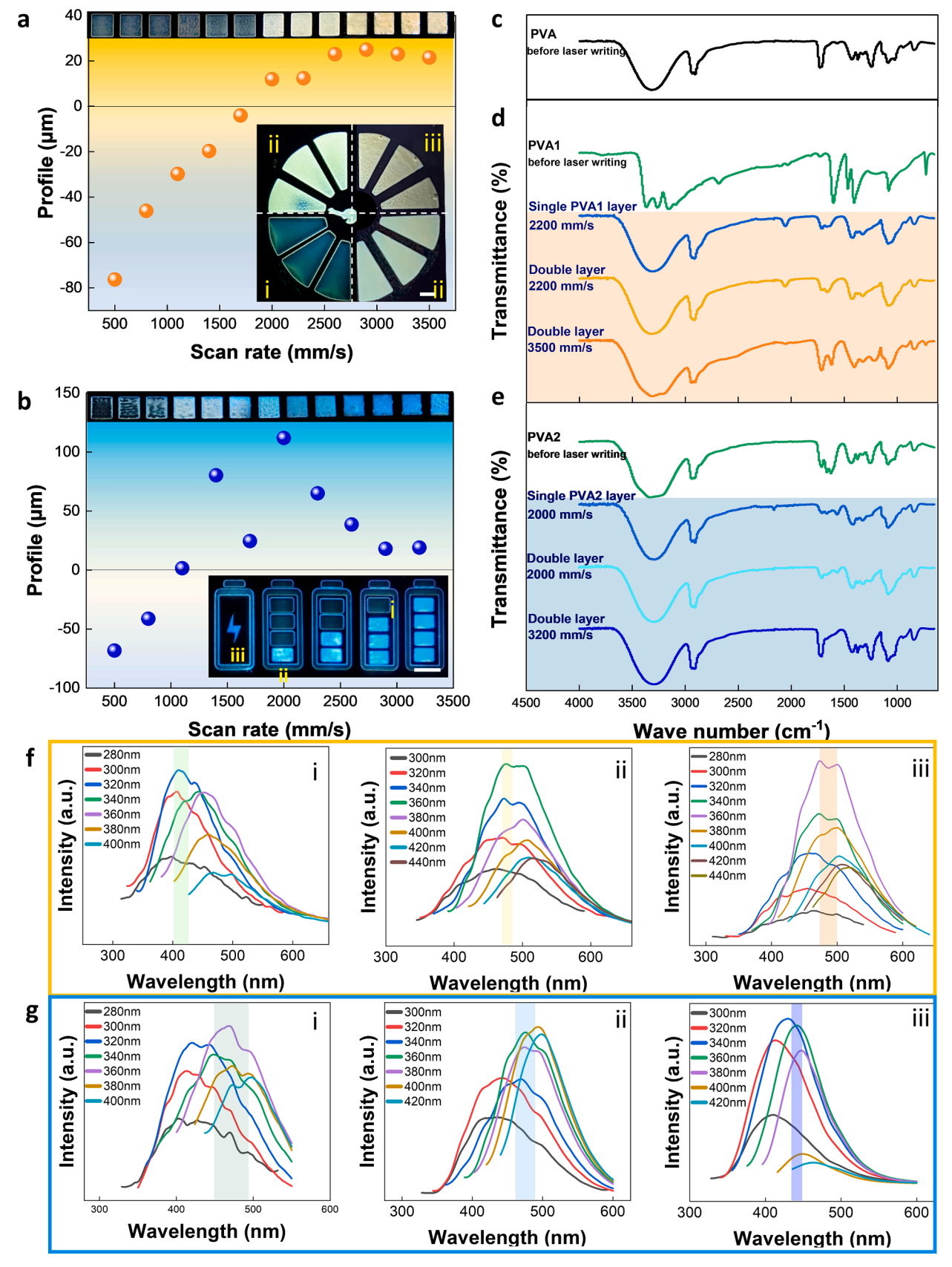


Fig. 1. The illustration of CO₂ laser writing fluorescent patterns on two distinct material platforms made by spin coating and freeze—thaw from composite PVA. **a**) On dual-layered composite polymer film of PVA1(PVA with citric acid/thiourea) /CAB and PVA2 (PVA with citric acid/urea)/CAB), the yellow, orange and blue squares present the laser patterned areas under made under different laser scanning rate, and the sample pictures taken under 365 nm UV light exhibited the flexibility of the self-standing patterned films, (the scale bar was 5 mm). **b**) On the PVA1 and PVA2 hydrogel, the photographs shown laser patterned hydrogels with yellow and blue squares under different laser parameters under 365 nm UV light, (the scale bar was 5 mm). (For interpretation of the references to color in this figure legend, the reader is referred to the web version of this article.)



(caption on next page)

Fig. 2. a) The surface profile of fluorescent squares made by *in situ* laser writing at scanning rate from 500 to 3500 mm/s on the surface of dual-layer PVA1/CAB film, the inset showed a fluorescent "wheel" image. The different fluorescent color areas on the "wheel" were made at different laser scanning rate (i at 1000 mm/s, ii at 2200 mm/s and iii at 3500 mm/s separately). The scale bar is 5 mm. b) The surface profile of fluorescent squares made by *in situ* laser writing at scanning rate from 500 to 3500 mm/s on dual-layer PVA2/CAB film, the inset showed a fluorescent label indicating battery level. The different fluorescent color areas were made at different laser scanning rate (i at 900 mm/s, ii at 2000 mm/s and iii at 3200 mm/s respectively). The scale bar is 5 mm. c) The FT-IR spectrum of pure PVA film. d) The comparison of FT-IR spectrum between single layer PVA1/CAB film by laser writing at scanning rate of 2200 mm/s and 3500 mm/s. e) The comparison of FT-IR spectrum between single layer PVA2 film before and after laser writing, and the FT-IR spectrum of fluorescent pattens on dual-layer PVA2/CAB film by laser writing at scanning rate of 2000 mm/s and 3200 mm/s. f-g) The solid fluorescence spectra of the i-iii area in the "wheel" and the battery level indicator label (the inset in Fig. 2a and be).

thermochemical reaction on the single layer and double layer structure were testified by the Fourier Transform Infrared Spectroscopy (FTIR) (Fig. 2d and Fig. S5). The FTIR spectra of laser-written single and double layers at 3500 mm/s were identical. In addition to the characteristic peaks associated with pure PVA, vibrational modes corresponding to C $= N (1620 \text{ cm}^{-1}), \text{ C-N } (1420 \text{ cm}^{-1}), \text{ and N-H } (3210 \text{ cm}^{-1}), \text{ indicative of }$ CDs synthesized from citric acid/thiourea (molar ratio 1:3.6, total concentration 20 wt% in PVA solution), were discerned in both single and double-layer film structures. Notably, the stretching vibrations of C-S, C = S, and SO₃H were identified by an absorption peak ranging between 1030 to 1220 cm⁻¹ at higher scan rates [35]. The reduction of the C = O(1710 cm⁻¹) bond on the surface of CDs at a lower scan rate suggested the increased carbonation. The presence of a peak at 2050 cm⁻¹ indicated the -NCS structure, derived from one of the thermal decomposition products of thiourea (isothiocyanic acid) [36]. Notably, the fluorescence turned to yellow as the -C-S bond decreased at lower laser scanning rate. An increase in the number of S can diminish the energy band gap between the highest occupied molecular orbital (HOMO) and the lowest unoccupied molecular orbital (LUMO), resulting in surface defects that act as energy traps, further contributing to the redshift of the emission wavelength [37,38]. This suggested that with reduced radiation energy (at high scan rate), the increased sulphur content in the CDs induced a redshift, resulting in an orange fluorescence color.

After laser writing, the patterned films (CD-Y@PVA1/CAB) with double layer structure detached from the glass substrate, yielding flexible, self-standing fluorescent patterned film (Fig. 1). The detachment was primarily attributed to the weak adhesion of cellulose acetate butyrate (CAB) on glass. Such a characteristic presented significant potential for anti-counterfeiting packaging materials, especially considering the inherent advantages of CAB material in packaging applications, such as high transparency and durable weather resistance.

To verify the universality of this method, the same strategy for making colorful patterns was also testified with the hydrogel made from solution 1 by the freeze-drying method (Fig. 1). From scan rate 800 to 3400 mm/s, bright yellow fluorescent patterns (CD-Y@PVA1) can be created on the surface of hydrogel. Different from double layer film, no change of fluorescent color was observed. The hydrogel films could be readily detached from the glass surface then adhered well to the skin, and the fluorescence of the pattern on hydrogel remain constant during stretching (Fig. S6b-c, SI move). The flexible self-standing fluorescent patterned hydrogel film would have potential applications on anti-counterfeiting of electronic skin or biosensor.

By varying the CDs precursor (citric acid/urea molar ratio 1:10, total concentration 3.6 wt% in PVA solution) in PVA film (PVA2), the color of the fluorescent pattern can be regulated to blue. The composite PVA film (PVA2) and PVA2 hydrogel were prepared after spin coating and freeze–thaw (Fig. 1). The absorption of 10.6 μ m CO₂ laser played a pivotal role in converting infrared (IR) photon energy, exciting the reactants into a vibrational state, and facilitating *in situ* CDs formation within the molten polymer matrix (Fig. S1b). On the double layer film surface, the fluorescence patterns (CD-B@PVA2/CAB) can be draw by CO₂ laser within the scan rate 800–3200 mm/s (Fig. 2b). The fluorescent intensity of the blue patterns (CD-B@PVA2) on hydrogel was less than on the composite PVA dry film. For double layer film structure, under high laser energy (800–1000 mm/s), the PVA2 layer almost completely pyrolysis. CDs were formed *in situ* within the CAB layer through the

pyrolysis of CAB molecules while the laser reached CAB layer, resulting in a light yellow-green fluorescence pattern (Fig. 2bi, g). Elevating the scan rate to 1200-2000 mm/s induced a transition in fluorescence from yellow-green to light blue (Fig. 2b). While the scan rate excessed 1000 mm/s, bubbles were formed in PVA2 layer during laser writing process, and the CD-B@PVA2/CAB film thickness increased (Fig. 2b). As the scan rate reached 2200 to 3200 mm/s, a stable bright blue was observed. The solid phase fluorescent has excitation dependent properties also indicating that the CDs were the source of the emission fluoresce (Fig. 2g). The CD-B@PVA2/CAB film thickness decreased again, when the scan rate over 2200 mm/s simply because that the lower laser energy at high scan rate was not high enough to melt composite PVA film. The laserwritten single-layer PVA2 film and double-layer PVA2/CAB were characterized by FT-IR individually (Fig. 2e). The asymmetric stretching vibration of N-H cannot be distinguished from the O-H between 3200 to 3500 cm⁻¹ due to overlapping. At a scan rate of 2000 mm/s, the bending vibration peak of urea amide groups manifested between 1650 to 1620 cm⁻¹, along with the vibration of C-N around 1430 cm⁻¹. Increasing the scan rate to 3000 mm/s, led to an increase in the tension vibrations of O-C = O, sp³ C-H, and the C-NH-C groups at 2713, 1373, and 1243 cm⁻¹ respectively. The increased N doping in CDs induced the blue shift emission. Similarly, flexible CD-B@PVA2/CAB film can be obtained after detaching from the glass substrate, and the flexible blue fluorescence patterned hydrogel can be formed by laser drawing on PVA2 hydrogel surface under scan rate 800-3600 mm/s (Fig. 1).

Different from the preparation of fluorescent composite polymer film by the physical mixing of CDs and polymers, the fluorescent color of the patterns cannot be regulated from yellow to red orange by altering the molar ratio of citric acid/urea or the laser writing parameters. It was known that the red CDs synthesized from citric acid/urea possess a bigger carbon core size with fewer surface functional groups, which was very challenge for laser-induced synthesis technology [39].

The multi-fluoresce color cannot be generated by mixing the three components together in a PVA solution, due to the similarity in laser energy requirements for producing distinct fluorescence colors and the low selectivity for laser-induced reactions within this system. To solve this problem, a multi-layer structure was constructed for making multicolor fluorescent patterns, as depicted in Fig. 3. A thin CAB layer (1 $\pm~0.2~\mu m)$ was strategically introduced between two-layer of PVA composite polymer films to prevent reactant mixing during drying steps.

Due to changes in structure and composition, the thermal conductivity would be changed with a multilayer structure, thus higher radiation energy was needed to draw through each layer. Varied fluoresce colors, blue, yellow orange and red orange were successfully achieved at scan rates of 3300 mm/s, 2200 mm/s, 1000 mm/s, and 500 mm/s, respectively (Fig. 3a, b). When considering an equivalent area of 0.5 mm², both the total scan time and the surface temperature increased with reducing scan rate (Fig. 5b). At a higher scan rate of 3300 mm/s, the thermal-chemical reaction exclusively occurred within the top layer (PVA2) during laser writing, resulting in the creation of a blue color (Fig. 3di). The maximum emission wavelength was around 450 nm. Under laser radiation, the composite PVA2 film underwent molten, expansion and gasification, creating noticeable bubbles between PVA2 and thin CAB layer, a phenomenon more obvious in the multilayer film structure. The gas bubbles formed during laser writing caused increasing of surface roughness, and the surface morphology of the film after laser

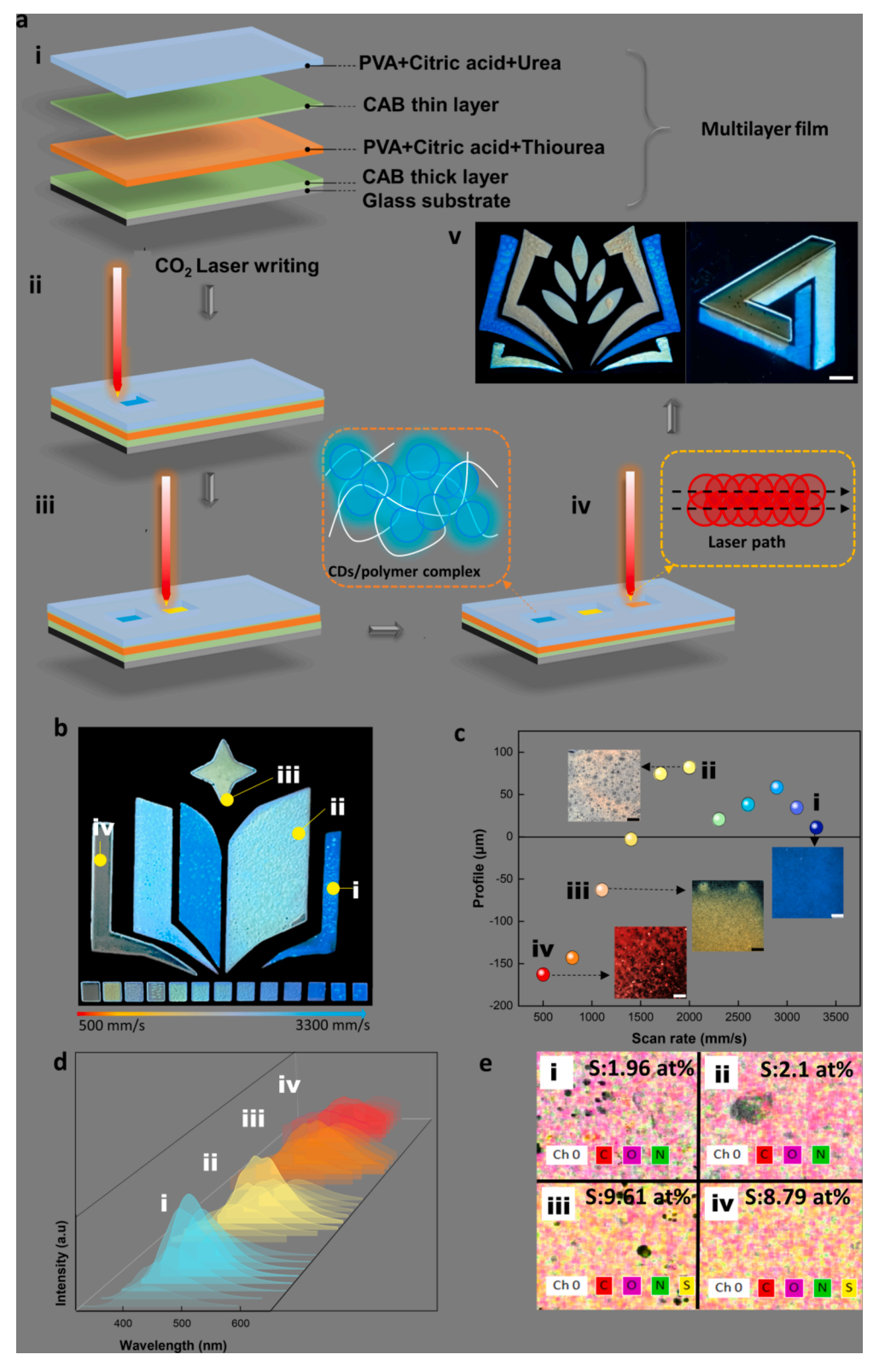


Fig. 3. a) Illustration of *in situ* fabrication multi-color fluorescent patterns on composite polymer film by CO₂ laser writing. The insets showed the schematic diagram of microstructure in the fluorescent pattern and laser path. Inset v showed the images of multicolor fluoresce patterns by *in situ* laser writing on monolithic composite polymer film with multilayer structure under 365 nm UV light. b) A colorful fluorescent pattern drawn *in situ* on composite film by CO₂ laser. The scale bar is 5 mm, the inset showed the fluorescent squares (5 mm²) made by laser writing at laser scanning rates from 500 mm/s to 3300 mm/s. c) The surface profile of fluorescent patterns made at laser scanning rate from 500 to 3300 mm/s, where the point i, ii, iii, vi corresponds to area i, ii, iii, vi, and the insets showed the fluorescence microscope pictures of each area, the scale bar is 500 μm. d) The solid fluorescent spectra of blue, yellow, orange and red orange area in the book image made at laser scanning rates of 3300, 2000, 1000, and 500 mm/s respectively, the excitation wavelength range from 300 nm to 420 nm for each fluorescent color. e) The EDS of i, ii, iii, vi area. (For interpretation of the references to color in this figure legend, the reader is referred to the web version of this article.)

writing was more convex than the original (Fig. 3c and Fig. S2). As the laser scanning rate decreased from 3300 mm/s to 500 mm/s, a gradual change in the fluorescent coloration of the squares depicted in Fig. 4a was observed. Specifically, as the laser scanning rate was reduced, the etching depth of the laser increased, leading to the gradual scorching and eventual complete vaporization of the PAV2 layer. Upon reaching the CAB layer, the formation of yellow-green CDsin the intermediate CAB layer was also noted [31]. Consequently, the resultant integration of the yellow-green CDs from the CAB and blue CDs from PAV2 layers produced a comprehensive color, which appeared the final transitional fluorescent color. Furthermore, with a continued decrease in the laser scanning rate, and as the removal of PAV2 was completed, a new transitional color emerged from the integration of yellow-green CDs originating from the first intermediate CAB and orange CDs from PAV1 layers. This color transition persisted until the complete removal of the first intermediate CAB layer. The generation of a fluorescent yellow pattern was achieved through the simultaneous formation of CDs on the top layer and the inter-media thin CAB layer within the melted matrix, exhibiting a maximum emission at approximately 480 nm (Fig. 3dii). The surface morphology did not change too much while the scan rate decreased from 3300 to 2200 mm/s. As the scan rate was further reduced to 1000 mm/s, the laser burned through the inter-media CAB layer and the accumulated heat energy facilitated the formation of CDs from citric acid/thiourea in the middle layer, resulting in an increased sulphur content and patterns exhibiting an orange color (Fig. 3d).

The maximum emission was around 480 nm with broad emission band over 500 nm. The surface temperature reached approximately 350 $^{\circ}$ C at scan rate 500 mm/s, leading to the decomposition of all layers except the base CAB layer (Fig. 5b). At a laser scanning rate of 500 mm/s, the laser penetrated to the bottom CAB layer. According to our

previous report, the fluorescent pattern produced by laser writing on CAB is expected to exhibit a greenish-yellow hue. However, in the case of the multilayer structured film, we observed that the fluorescent pattern on the bottom CAB layer appeared red-orange. Energy Dispersive Spectroscopy (EDS) analysis of the patterned area revealed the presence of not only C and O but also N and S on the patterned surface (Fig. S7d). Based on these findings, we propose that the darker fluorescent color arises not only from the extending of thermal reaction but also from the retaining of the nitrogen and sulfur atoms those initially existed in the overlying layers and were incorporated into the CDs during the pyrolysis of the CAB layer. (Fig. S7d). The maximum emission shift to 500 nm and the broad emission band over 550 nm (Fig. 3div). The etching depth increased while the laser scan rate less than 1400 mm/s, the laser written surface became smooth when the scan rate less than 1000 mm/s.

Therefore, by adjusting the laser scan rate, a diverse range of multicolor fluorescent patterns with different surface morphology can be intricately drawn on polymer composite film through the *in situ* formation of distinct CDs via infrared laser-induced thermal-chemical reactions. The distinctive fluorescence color and surface structure imparted non-replicable characteristics to the patterns, rendering the patterns particularly suitable for applications in anti-counterfeiting. In addition, fluorescent patterns fabricated via laser direct writing exhibit remarkable photostability, retaining their luminescence for up to 24 months under indoor conditions (Fig. 4a). Our experimental results reveal that while the absolute quantum efficiency of CD-B@PVA2/CAB film surpasses that of other colors, their rate of fluorescence decay is also higher, with yellow patterns demonstrating superior stability. Furthermore, we discovered that applying an organosilicon polymer coating to the surface of the laser-written fluorescent patterns effectively stabilizes

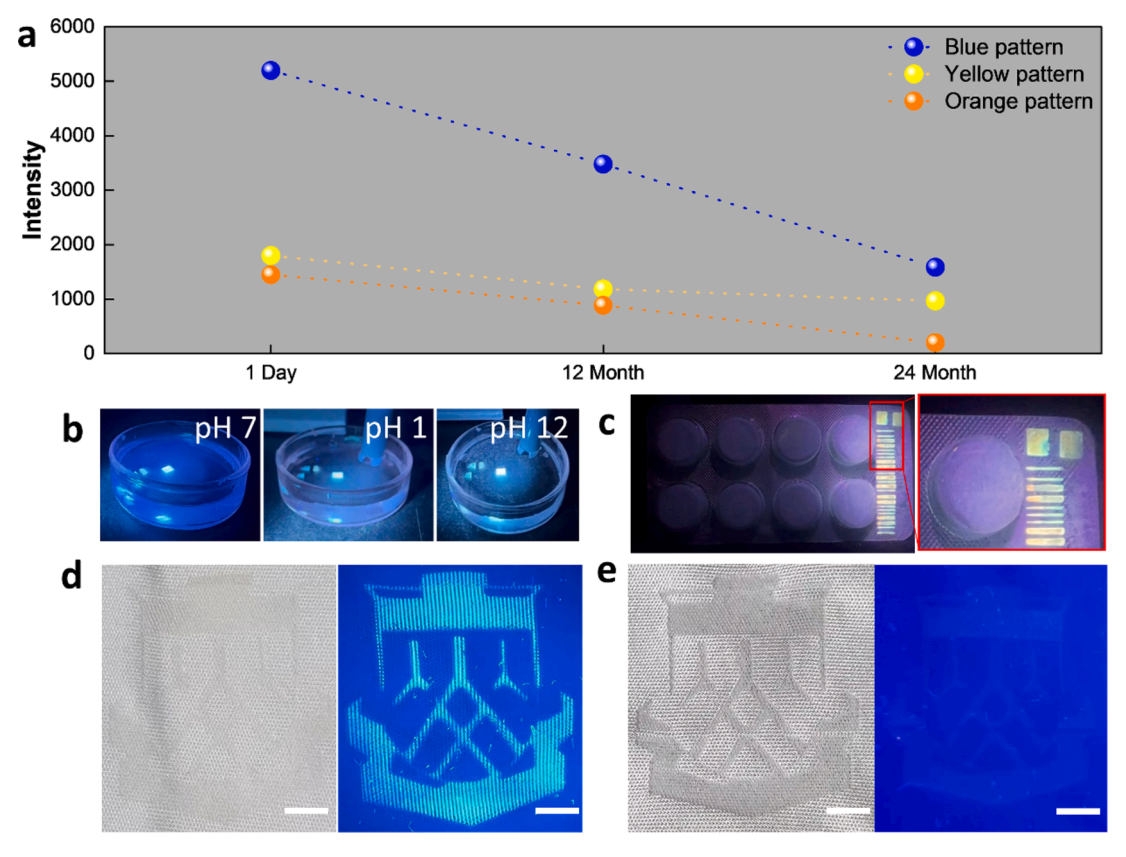


Fig. 4. a) The stability of the colorful pattern in the laboratory environment from 1 month to 24 month. b) The image of laser written blue fluorescent square (5 mm²) in water solution of pH 1, pH 7, and pH 12. c) The image of laser written fluorescent QR codes on pharmaceutical packaging with CAB/PVA1 coating and d) The image of laser written fluorescent SCNU school logo on a piece of textile with CAB/PVA2 coating under daylight and UV light. e) The image of laser written fluorescent SCNU school logo on a piece of textile without CAB/PVA2 coating under daylight and UV light. (For interpretation of the references to color in this figure legend, the reader is referred to the web version of this article.)

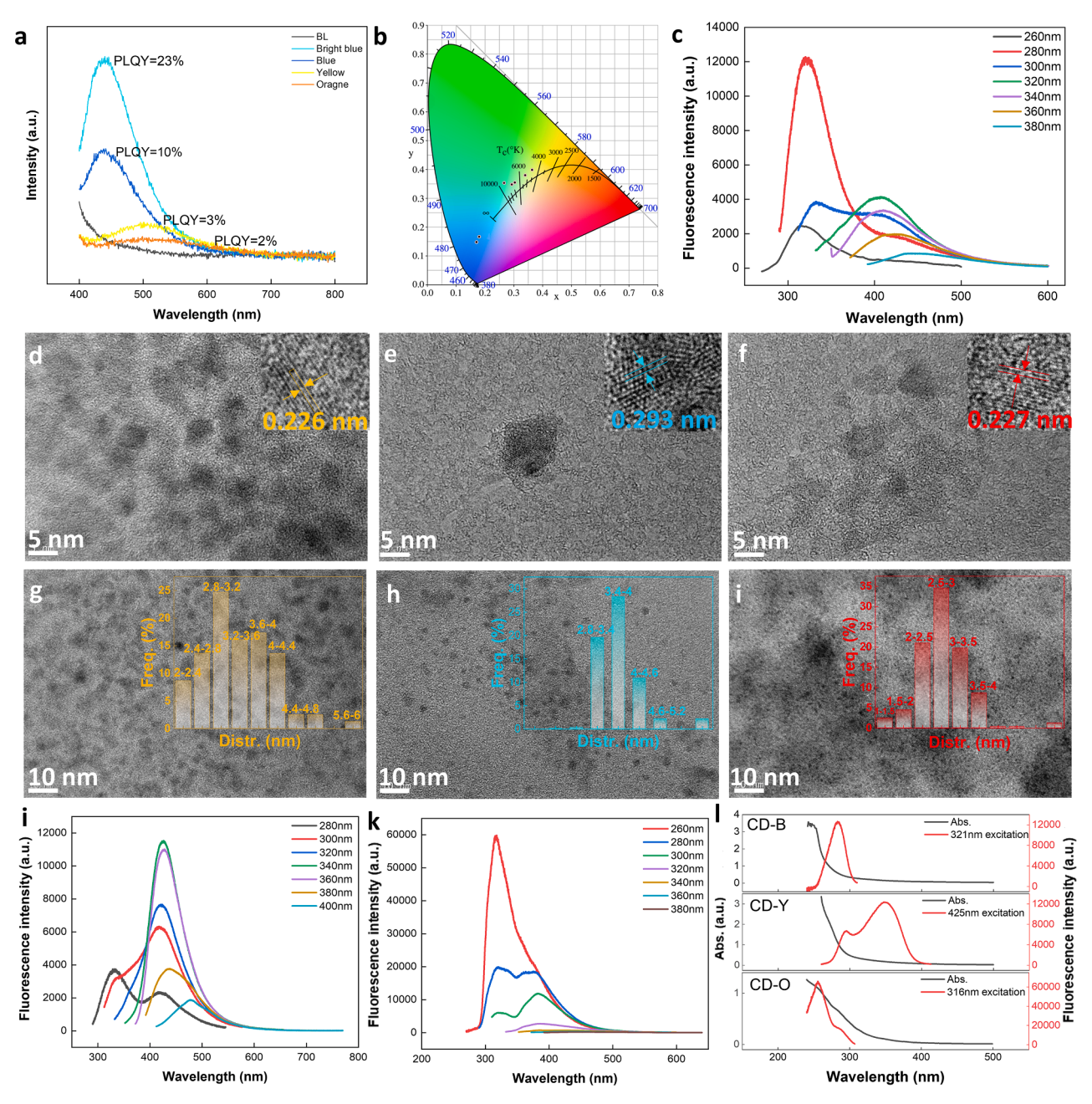


Fig. 5. a) The absolute quantum efficiency and b) The CIE color coordinate of blue, yellow and orange fluorescent patterns. c) The FL spectra of CD-B solution. d-f) The HRTEM images of CD-Y, CD-B and CD-O at 400 k, the insets showed the crystalline space in single CDs. g-i) The TEM images of CD-Y, CD-B and CD-O at 200 k, the insets showed the CDs size distribution. j-k) The FL spectra of CD-Y and CD-O solution. l) UV-vis and FL excitation spectra of CD-B, CD-Y, and CD-O. (For interpretation of the references to color in this figure legend, the reader is referred to the web version of this article.)

them in aqueous solutions with pH values of 1, 7, and 12 (Fig. 4b).

Beyond the use of spin-coating for the fabrication of high-precision colored fluorescent patterns, our study suggests that for applications with lower precision requirements, simple dip-coating or blade-coating techniques can be employed. These methods allow for the deposition of pre-formulated CAB, PVA1, and PVA2 onto target surfaces, streamlining the production of fluorescent markers. Notably, due to the favourable biocompatibility of the selected materials, this coating can be applied to pharmaceutical packaging or textiles (Fig. 4c). Following a straightforward drying process and laser direct writing, fluorescent QR (quick response code) codes and specific pattern markers can be readily achieved.

In summary, our findings further validate the broad applicability of the proposed method for fabricating colored fluorescent patterns, highlighting its potential for diverse practical applications.

In addition, under 365 nm UV light, all colors were distinguishable, and the absolute quantum efficiency at 365 nm was quantified. As depicted in Fig. 5a, the highest absolute quantum efficiency for the blue color reached 23 %. The robust intermolecular interaction between N-H on CDs and OH on the PVA matrix significantly enhanced the blue fluorescence quantum yield. Further validation of the color transition from orange, yellow to blue under 365 nm UV was evident in the CIE coordinates (Fig. 5b).

3.2. Characterization of CDs from the fluorescent patterns

To identify the CDs generated during laser writing within the patterned area, the patterns were immersed in OR water at room

temperature for one week. The CDs solution was obtained through dialysis and centrifugation. The TEM images revealed that the average size of CDs varied from 2.9 nm (from orange pattern) to 3.35 nm (from yellow pattern), all with crystalline structure. The lattice spacing was almost the same for the CD-Y (0.226 nm, from yellow pattern) and CD-O (0.227 nm, from orange pattern), where the lattice spacing of CD-B (from blue pattern) was the largest (0.293 nm) and it had a wide size distribution (Fig. 5g-i). The broad size distribution of the CDs synthesized in our study leads to a diversity of energy band structures, resulting in distinct absorption and emission characteristics based on size, which further influences excitation dependence [40]. The fluorescence spectrum of the CD-Y solution demonstrated an excitation-dependent property, with the maximum excitation wavelength recorded at 425 nm (Fig. 5j). And the maximum excitation wavelength for CD-O was observed at 316 nm (Fig. 5l).

Similarly with CD-Y, the CD-B solution derived from the blue pattern showed excitation dependency, with the maximum excitation wavelength measured at 321 nm (Fig. 51). Doping with N altered the distribution of surface states within the CDs, affecting their fluorescence emission properties, electronic structures, and energy level distributions of different surface states, all of which contribute to the observed excitation dependence [41]. From the high-resolution transmission electron microscopy, there was a blur shell without a crystal structure around the CDs. The CD-Y solution exhibited no obvious $n-\pi^*$ or $\pi-\pi^*$ conjugation peak in the UV-vis spectrum, which could be attributed to the polymer chain grafting onto the surface of the CDs during growth or the formation of a polymer shell due to hydrogen bonding between the CDs and Polyvinyl Alcohol (PVA). Especially, in the solution of CD-B, the presence of large particles indicated the existence of a polymer shell grafted outside the CDs, explaining the high absolute quantum efficiency of the fluorescence pattern (Fig. S8b). The incorporation of PVA chains effectively mitigated the aggregation of CDs, thereby enhancing the absolute quantum yield. The interaction between the CDs and the PVA matrix also affected the fluorescence properties. This interaction may modify the electronic structure and energy level distribution of the CDs, thereby further contributing to the excitation dependence. In comparison, the generation of orange patterns, facilitated by higher laser energy and an extended thermal-chemical reaction time, resulted in small particle size without shell under more thorough carbonization (Fig. S8a). The π - π * conjugation peak at 320 nm in the UV–vis spectrum can be determined (Fig. 51). The hydrogen bonding between the CDs and the PVA matrix was examined by FT-IR with increasing temperature (Fig. S10 b-d). In the FTIR spectrum, hydrogen-bonded O-H stretching vibrations typically appear as broader peaks (around 3300 cm⁻¹). As temperature increases, we observed a shift in the O-H stretching peak to higher frequencies (higher wave number) as hydrogen bonds weaken in blue fluorescent pattern which indicated the broken of hydrogen bonds between CDs and PVA [42]. A reduction in hydrogen bond strength results in a lesser extent of dipole-dipole interaction, which could impact the intensity of the corresponding peak. The intensity of the O-H stretching band decreased with increasing temperature as the extent of hydrogen bonding decreases. There was a similarly trend in yellow and orange pattern, and the shoulder peaks are also more pronounced in the higher bands. In addition, the peak around 2400 \mbox{cm}^{-1} belonged to the CO₂ in the test environment. DSC of the fluorescent patterns and PAV1, PAV2 were also tested to verify the presence of hydrogen bonding between CDs and polymer matrix [43]. The increasing Tg of CD-B@PAV2 and decreasing Tg of CD-O@PVA1 related with change of hydrogen bonds in blue and orange patterns after laser writing, which corresponding to the absolute quantum efficiency (Fig. S10 e-h).

The X-ray photoelectron spectroscopy analysis of CDs from the three-colour fluorescent patterns was presented in Fig. S9. Due to the presence of thiourea in the reactants, the compositions of CD-Y and CD-O were essentially similar, comprising C, O, N, and S. And the blue CDs consisted of C, O, and N. As the laser scanning speed decreased from 3500 to 1000 mm/s, the polymer surface obtained higher energy, leading to an

increase in surface temperature. With the increasing of surface reaction temperature and reaction time, the carbon content raised from 67.88 % to 67.99 %, oxygen content decreased from 23.13 % to 22.86 %, and nitrogen content increased from 6.1 to 6.63 % (Tables S2, S3). C-C/C = C, C-N, C-O, C-S, and C = C/C = O were the main types carbon in CDs. Compared to CD-Y, the carbon content in CD-O was slightly higher, with a noticeable increased in graphitic carbon content, indicating a higher degree of graphitization. Besides sulphur, nitrogen elements predominantly consisted of pyridinic nitrogen (399.2 eV), pyrrolic nitrogen (400.7 eV), and graphitic nitrogen (401.7 eV). As reaction time and temperature increased, the content of pyrrolic nitrogen rose while the content of pyridinic nitrogen decreased. The high radiation energy led to the removal of polymer segments from the surface of CDs, resulting in a corresponding decrease in C-O content. The average size of CD-O was smaller than CD-Y, and the particle size distribution was more uniform that was consistent with the XPS results. The redshift in the fluorescence color of CDs was attributed to sulphur element doping. The content of C-S in CD-Y and CD-O was essentially the same, indicating that the redshift in the orange color could be attributed to a higher degree of carbonization in the CDs. Additionally, a peak around 165.8 eV revealed the presence of sulfate ions (at the end of the molecular chain) or sulfite ions (in the middle of the molecular chain) in the fluorescent pattern, which mainly originating from urea sulphur in the reactants.

The blue fluorescence pattern was obtained at higher scanning rates, and the average radiation temperature on the material surface during the preparation process was relatively low. The CD-B contained pyridine nitrogen, pyrrole nitrogen, etc (Fig. S9). According to the literature, nitrogen doping can enhances the surface characteristics of CDs, alter the electronic and energy band structure as well as the conjugation system and the introduction of heteroatomic jumps within the molecular framework which would result in a blue shift of the fluorescence emission peaks [44]. In CD-B, the oxygen content was higher than in CD-Y and CD-O, indicating a greater presence of oxygen functional groups on the surface of the CD-B. These additional functional groups were likely derived from the PVA molecules serving as reaction media. The functional groups encapsulated on the surface of CD-B effectively mitigated fluorescence quenching, allowing the blue fluorescence to achieve a high absolute quantum yield. The XRD was examined to analyze the degree of graphitization (Fig. S10). There were broad peak appeared at around 25° for all three CDs which should correspond to the 002 crystal plane and also provided the interlayer spacing information in graphitic materials. The broad peak indicated the highly disordered carbon atoms and a lower degree of graphitization.

3.3. Thermodynamic analysis of the laser direct writing process for fluorescent pattern fabrication

In liquid-phase CDs synthesis reactions, molecules were activated under high-temperature and high-pressure conditions, leading to chemical reactions between activated functional groups of different reactants, followed by further carbonization to produce CDs. Apart from liquid phase reaction, the synthesis of CDs using two solid reactants had been demonstrated to be able to exhibit solid-state fluorescence properties. Normally, solid phase reactions involved the catalytic synthesis and carbonization of materials under high-temperature and highpressure conditions, with the addition of inert dispersants. However, the mechanisms behind laser-induced CDs formation in solid polymerdoped systems have been reported with unclear clarity. Generally, the reactive species can be produced by laser-powered homogeneous pyrolysis (LPHP) of a single precursor through photosensitization such as by sulphur hexafluoride, or by thermal chemistry in binary mixtures initiated via infrared multiphoton excitation and decomposition of one component [26,45]. The utilization of the IR laser technique proved highly effective in the creation of innovative organic and organometallic polymeric coatings. For CO₂ lasers, the process was primarily governed by thermal absorption. The energy transfer can also occur through

multi-photon absorption or avalanche ionization processes. Chemical reactions induced by a single laser, where the irradiating wavelength was absorbed by one of two distinct reactants, can manifest through three distinct mechanisms. Firstly, primary dissociation of the absorbing species takes place, leading to subsequent reactions of the resulting products. The second mechanism involved a photosensitized process, while the third was a mode induced through reactive collisions between both energized reactants.

Citric acid, urea, and thiourea were chosen as CDs precursors in PVA since the performance of the synthesis CDs by solvent-thermal reactions can be manipulated by changing reaction temperatures and times. As we noticed, the pure PVA exhibited no fluorescence within the utilized laser scan rate range. This not only benefited that the patterned fluorescence colors remain distinct between different layers, but also indicated that the CDs formed during laser writing were mainly due to the laser induce reaction of CDs precursors. The hydroxyl groups on PVA polymer chains formed hydrogen bonds with the amino and carboxyl groups of urea, thiourea, and citric acid [46]. This interaction played a crucial role in ensuring the laser-induced reactions of small molecules within the PVA film matrix (Fig. 6).

Firstly, the intermolecular interactions between PVA and CDs precursors facilitated the uniform dispersion of the precursors within the PVA network, preventing the recrystallization and precipitation during film formation. During laser writing, CDs can be uniformly generated and distributed in the laser radiation region on film surface. Secondly, the homogeneous dispersion of CDs precursors within the PVA films was crucial for effective laser-induced synthesis within micrometre-scale

regions. The uniform distribution of CDs precursors enhanced the laser-induced photochemical reaction efficiency, which in turn promoted the CDs dispersion the PVA film matrix, yielding fluorescent patterns exhibiting elevated absolute quantum efficiency. In comparison, the colorful fluoresce cannot be observed if the PVA changed into CAB, which either due to the generation of CDs from CAB itself that potentially obstructing the visibility of other fluorescence colors, or due to the inefficiently distribution of CDs precursors in CAB. This indirectly corroborated the importance of hydrogen bonding in promoting the formation of fluorescent patterns.

During laser writing process, both types of doped PVA materials exhibited two thermal decomposition reaction stages (Fig. S11). For PVA1, the first reaction stage occurred around 350 °C, primarily involving the thermal decomposition of PVA and the reaction between citric acid and thiourea molecules. The second stage occurred around 450 °C, corresponding to the carbonization process. In the case of PVA2, the first stage occurred at around 220 °C, and the second stage occurred at around 400 °C, indicating slightly lower reaction energy requirements than PVA1. Additionally, the temperature of photochemical reactions decreased with an increase in the amount of small molecules in PVA (Fig. S12). The glass transition temperature (Tg) of PVA1 and PVA2 also decreased with an increase in the quantity of the CDs precursors (Fig. S13).

Lower thermodynamic reaction temperatures suggested that more molecules could be activated at the same temperature, and the chemical reactions of CDs precursors more efficient. By measuring TGA curves at different heating rates and employing the Flynn-Wall-Ozawa method

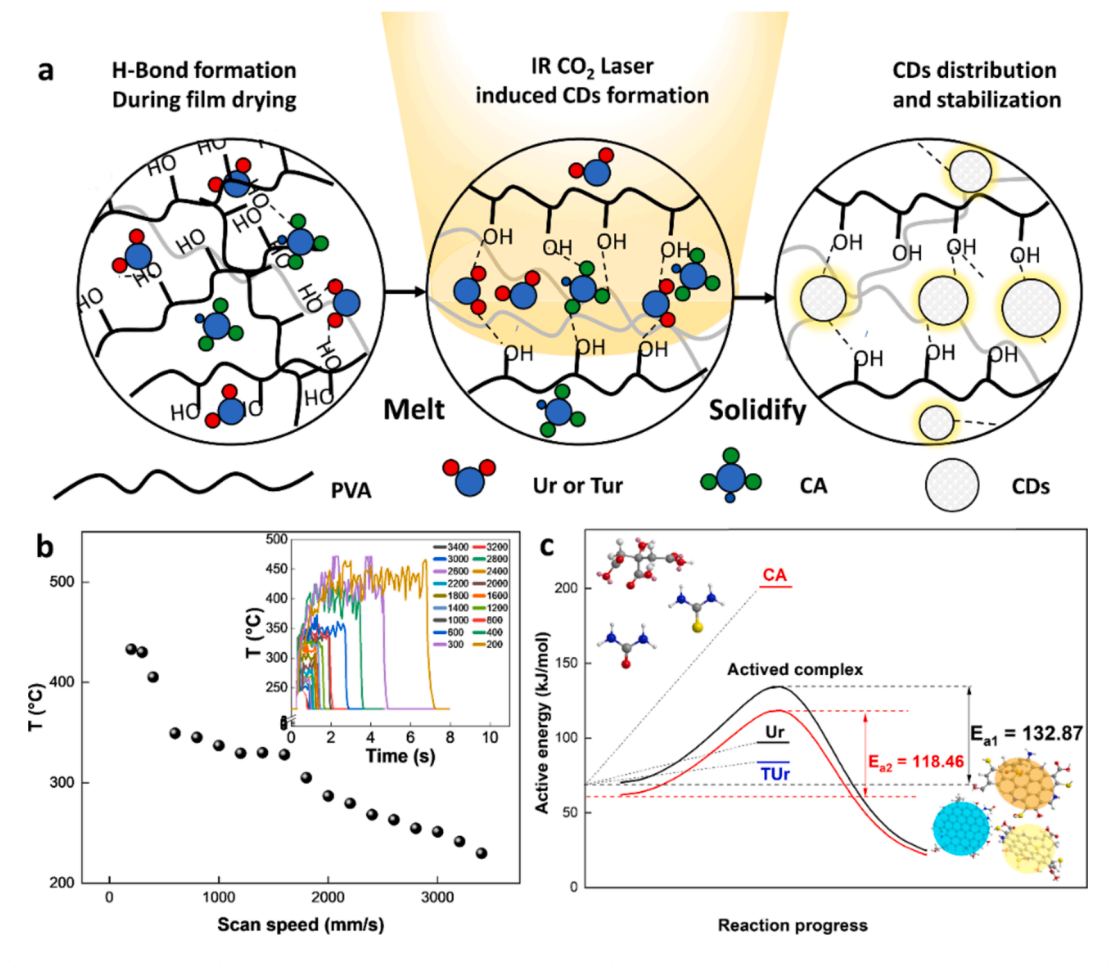


Fig. 6. A) The illustration of intermolecular force influence between polymer chain and the precursor of CDs on CO_2 laser induced photochemical reaction. b) The surface temperature during laser writing on composite film while making multicolor fluorescence patterns, the insets showed the temperature curve during laser writing process at different scanning rates. c) The illustration of active energy change occurring during photo-thermal reaction under laser writing process, the active energy of citric acid (CA), urea (Ur) and thiourea (Tur) were referred to the literature of [36,47 and 48].

along with ASTM E1641-2018 standards, the reaction activation energies for the PVA1 and PVA2 were determined to be 132.87 and 118.46 kJ/mol, respectively [49]. The total laser radiation energy during the laser writing process (with a single laser pulse energy density of 122 J/mm2 and 25,000 pulses per second) significantly surpasses the required activation energy for the reactions.

Therefore, the IR photo-induced synthesis of CDs from citric acid and thiourea, as well as citric acid and urea, can occur within the molten PVA polymer. Under the radiation of laser in composite PVA, the material initially reached a molten state. In this molten state, the reactive groups of small molecules vibrated intensively upon absorbing photons. Upon surpassing the activation energy barrier, chemical reactions could occur among molecules. Subsequently, as the absorbed energy continued to increase, the material underwent carbonization, leading to the formation of CDs. During the photochemical reaction process, PVA molecular chains actively participated in the reaction, grafting onto the surface of the CDs. This involvement to some extent played a role in separating the CDs. In the irradiation of CO₂ laser processing, the surface temperature of the polymer film increased as the scanning rate decreased, reaching a maximum temperature of around 450 °C. At this temperature, the residual material was approximately 20 %, indicating that most of the material was gasified at high temperatures (Fig. S11). TEM analysis indicated that CD-O were smaller in size compared to CD-B due to more completely carbonization. Consequently, the functional groups on the surface of the obtained CDs were reduced, and fluorescence mainly originates from the conjugated structure of the carbon core. Since the higher laser energy has to be used for generation CD-O, which will largely reduce the amounts of functional groups on the surface, the aggregation of CD-O is more likely to occur in PVA, resulting in decreasing of absolute quantum efficiency [16].

4. Conclusions

In conclusion, our study presented a versatile and efficient method for the fabrication of multicolor fluorescent color (blue, yellow and orange) in one pattern on the solid polymer films, hydrogel surface using IR CO₂ laser writing. Our fluorescent patterning methodology can efficiently finish a 5 cm2 colorful pattern within 5 min with line width accuracy up to 300 μm . This study unveiled the thermal dynamics governing the laser-induced formation of CDs in doped PVA polymer. The interaction between PVA molecular chains and CDs precursors before laser induces photochemical reaction ensuring the homogenously formation of CDs, together with the interaction between PVA chain and CDs contributes to the high absolute quantum yield (23 %). This indepth understanding of the photochemical reactions and thermal kinetics provided a foundation for further exploration and optimization of the synthesis conditions, opening avenues for tailored applications in diverse fields such as optoelectronics and biomedicine. The universality of this approach was testified by fabricating fluorescent QR code and school logo on pharmaceutical packaging and fabrics respectively. The tunability of fluorescence colors through precise control of reaction conditions, hierarchical structure of patterns and the physically unclonable surface morphology offered promising prospects for practical applications, particularly in anti-counterfeiting.

CRediT authorship contribution statement

Yuanyuan Guo: Writing – original draft. Yixun Gao: Resources. Yao Wang: Conceptualization. Yi-Kuen Lee: Investigation. Patrick J. French: Ahmad M. Umar Siddiqui: Writing – review & editing. Hao Li: Investigation. Guofu Zhou: Funding acquisition.

Declaration of competing interest

The authors declare that they have no known competing financial interests or personal relationships that could have appeared to influence the work reported in this paper.

Acknowledgments

This work was supported by the National Natural Science Foundation of China (Grant No. 51973070), Science and Technology Program of Guangzhou (No. 2019050001), Guangdong Provincial Key Laboratory of Optical Information Materials and Technology (2023B1212060065), MOE International Laboratory for Optical Information Technologies, the 111 Project, and the High–end Foreign Experts Recruitment Program (DL2023030001L).

Appendix A. Supplementary data

Supplementary data to this article can be found online at https://doi.org/10.1016/j.cej.2024.158749.

Data availability

No data was used for the research described in the article.

References

- [1] F. Yuan, Y.-K. Wang, G. Sharma, Y. Dong, X. Zheng, P. Li, A. Johnston, G. Bappi, J. Z. Fan, H. Kung, Bright high-colour-purity deep-blue carbon dot light-emitting diodes via efficient edge amination, Nat. Photonics 14 (3) (2020) 171–176.
- [2] Y. Zhang, J. Wang, L. Wang, R. Fu, L. Sui, H. Song, Y. Hu, S. Lu, Carbon dots with blue-to-near-infrared lasing for colorful speckle-free laser imaging and dynamical holographic display, Adv. Mater. 35 (31) (2023) 2302536.
- [3] C. Ji, Y. Zhou, R.M. Leblanc, Z. Peng, Recent developments of carbon dots in biosensing: a review, ACS Sens. 5 (9) (2020) 2724–2741.
- [4] H.Y. Wang, L. Zhou, H.M. Yu, X.D. Tang, C. Xing, G. Nie, H. Akafzade, S.Y. Wang, W. Chen, Exploration of room-temperature phosphorescence and new mechanism on carbon dots in a polyacrylamide platform and their applications for anti-counterfeiting and information encryption, Adv. Opt. Mater. 10 (15) (2022) 2200678
- [5] A. Segkos, I. Sakellis, N. Boukos, C. Drivas, S. Kennou, K. Kordatos, C. Tsamis, Patterned carbon dot-based thin films for solid-state devices, Nanoscale 12 (18) (2020) 10254–10264.
- [6] S. Jung, W.-L. Cheung, S.-J. Li, M. Wang, W. Li, C. Wang, X. Song, G. Wei, Q. Song, S.S. Chen, Enhancing operational stability of OLEDs based on subatomic modified thermally activated delayed fluorescence compounds, Nat. Commun. 14 (1) (2023) 6481.
- [7] Z. Li, X. Liu, G. Wang, B. Li, H. Chen, H. Li, Y. Zhao, Photoresponsive supramolecular coordination polyelectrolyte as smart anticounterfeiting inks, Nat. Commun. 12 (1) (2021) 1363.
- [8] J. Liu, R. Li, B. Yang, Carbon dots: a new type of carbon-based nanomaterial with wide applications, ACS Cent. Sci. 6 (12) (2020) 2179–2195.
- [9] B. Wang, S. Lu, The light of carbon dots: from mechanism to applications, Matter 5 (1) (2022) 110–149.
- [10] B. Wang, J. Yu, L. Sui, S. Zhu, Z. Tang, B. Yang, S. Lu, Rational design of multicolor-emissive carbon dots in a single reaction system by hydrothermal, Adv. Sci. 8 (1) (2021) 2001453.
- [11] H. Wang, L. Ai, H. Song, Z. Song, X. Yong, S. Qu, S. Lu, Innovations in the solid-state fluorescence of carbon dots: strategies, optical manipulations, and applications, Adv. Funct. Mater. 33 (41) (2023) 2303756.
- [12] S.K. Bhunia, S. Nandi, R. Shikler, R. Jelinek, Tuneable light-emitting carbon-dot/polymer flexible films prepared through one-pot synthesis, Nanoscale 8 (6) (2016) 3400–3406.
- [13] F. Lian, C. Wang, Q. Wu, M. Yang, Z. Wang, C. Zhang, In situ synthesis of stretchable and highly stable multi-color carbon-dots/polyurethane composite films for light-emitting devices, RSC Adv. 10 (3) (2020) 1281–1286.
- [14] J. Bai, G. Yuan, X. Chen, L. Zhang, Y. Zhu, X. Wang, L. Ren, Simple strategy for scalable preparation carbon dots: RTP, time-dependent fluorescence, and NIR behaviors, Adv. Sci. 9 (5) (2022) 2104278.
- [15] J. Ren, L. Stagi, P. Innocenzi, Fluorescent carbon dots in solid-state: from nanostructures to functional devices, Prog. Solid State Chem. 62 (2021) 100295.
- [16] L. Ai, Z. Song, M. Nie, J. Yu, F. Liu, H. Song, B. Zhang, G.I. Waterhouse, S. Lu, Solid-state fluorescence from carbon dots widely tunable from blue to deep red through surface ligand modulation, Angew. Chem. Int. Ed. 62 (12) (2023) e202217822.
- [17] S. Ma, H. Ma, K. Yang, Z. Tan, B. Zhao, J. Deng, Intense circularly polarized fluorescence and room-temperature phosphorescence in carbon dots/chiral helical polymer composite films, ACS Nano 17 (7) (2023) 6912–6921.
- [18] H.J. Li, Y. Chen, H. Wang, H. Wang, Q. Liao, S. Han, Y. Li, D. Wang, G. Li, Y. Deng, Amide (n, π*) transitions enabled clusteroluminescence in solid-state carbon dots, Adv. Funct. Mater. 33 (37) (2023) 2302862.
- [19] D. Zhou, Y. Zhai, S. Qu, D. Li, P. Jing, W. Ji, D. Shen, A.L. Rogach, Electrostatic assembly guided synthesis of highly luminescent carbon-nanodots@ BaSO₄ hybrid phosphors with improved stability, Small 13 (6) (2017) 1602055.

- [20] Y. Deng, Q. Li, Y. Zhou, J. Qian, Fully inkjet printing preparation of a carbon dots multichannel microfluidic paper-based sensor and its application in food additive detection, ACS Appl. Mater. Interfaces 13 (48) (2021) 57084–57091.
- [21] S.Y. Liang, Y.F. Liu, S.Y. Wang, Z.K. Ji, H. Xia, B.F. Bai, H.B. Sun, High-resolution patterning of 2D perovskite films through femtosecond laser direct writing, Adv. Funct. Mater. 32 (38) (2022) 0224957.
- [22] X. Huang, Q. Guo, D. Yang, X. Xiao, X. Liu, Z. Xia, F. Fan, J. Qiu, G. Dong, Reversible 3D laser printing of perovskite quantum dots inside a transparent medium, Nat. Photonics 14 (2) (2020) 82–88.
- [23] W. Zhan, L. Meng, C. Shao, X.-G. Wu, K. Shi, H. Zhong, In situ patterning perovskite quantum dots by direct laser writing fabrication, ACS Photonics 8 (3) (2021) 765–770
- [24] B. Senyuk, N. Behabtu, A. Martinez, T. Lee, D.E. Tsentalovich, G. Ceriotti, J. M. Tour, M. Pasquali, I.I. Smalyukh, Three-dimensional patterning of solid microstructures through laser reduction of colloidal graphene oxide in liquid-crystalline dispersions, Nat. Commun. 6 (2015) 7157.
- [25] W.C. Danen, Pulsed infrared laser-induced organic chemical reactions, Opt. Eng. 19 (1) (1980) 21–28.
- [26] J. Pola, CO2 laser-induced thermal chemical vapour deposition of polymers, J. Anal. Appl. Pyrol. 30 (1) (1994) 73–90.
- [27] W. Xiong, L. Jiang, T. Baldacchini, Y. Lu. Laser additive manufacturing using nanofabrication by integrated two-photon polymerization and multiphoton ablation, Laser Additive Manufacturing, Elsevier2017, pp. 237-256.
- [28] J. Wu, J.H. Lei, B. He, C.-X. Deng, Z. Tang, S. Qu, Generating long-wavelength absorption bands with enhanced deep red fluorescence and photothermal performance in fused carbon dots aggregates, Aggregate 2 (6) (2021) e139.
- [29] J. Yu, X. Yong, Z. Tang, B. Yang, S. Lu, Theoretical understanding of structure-property relationships in luminescence of carbon dots, J Phys. Chem. Lett. 12 (32) (2021) 7671–7687.
- [30] X. Li, H. Wang, Y. Shimizu, A. Pyatenko, K. Kawaguchi, N. Koshizaki, Preparation of carbon quantum dots with tunable photoluminescence by rapid laser passivation in ordinary organic solvents, Chem. Commun. 47 (3) (2010) 932–934.
- [31] Y. Guo, Q. Wang, H. Li, Y. Gao, X. Xu, B. Tang, Y. Wang, B. Yang, Y.-K. Lee, P. J. French, Carbon dots embedded in cellulose film: programmable, performance-tunable, and large-scale subtle fluorescent patterning by in situ laser writing, ACS Nano 16 (2) (2022) 2910–2920.
- [32] J. Zhang, Y. Liu, C. Njel, S. Ronneberger, N.V. Tarakina, F.F. Loeffler, An all-in-one nanoprinting approach for the synthesis of a nanofilm library for unclonable anticounterfeiting applications, Nat. Nanotechnol. 18 (2023) 1027–1035.
- [33] Y. Wang, T. Lv, K. Yin, N. Feng, X. Sun, J. Zhou, H. Li, Carbon dot-based hydrogels: preparations, properties, and applications, Small 19 (17) (2023) 2207048.
- [34] H. Liu, W. Lin, M. Hong, Hybrid laser precision engineering of transparent hard materials: challenges, solutions and applications, Light Sci. Appl. 10 (1) (2021)

- [35] Q. Wang, Y. Gao, B. Wang, Y. Guo, U. Ahmad, Y. Wang, Y. Wang, S. Lu, H. Li, G. Zhou, S, N-Codoped oil-soluble fluorescent carbon dots for a high colorrendering WLED, J. Mater. Chem. C 8 (13) (2020) 4343–4349.
- [36] S. Wang, Q. Gao, J. Wang, Thermodynamic analysis of decomposition of thiourea and thiourea oxides, J. Phys. Chem. B 109 (36) (2005) 17281–17289.
- [37] F. Yan, Z. Sun, H. Zhang, X. Sun, Y. Jiang, Z. Bai, The fluorescence mechanism of carbon dots, and methods for tuning their emission color: a review, Microchim. Acta 186 (8) (2019) 583.
- [38] X. Miao, X. Yan, D. Qu, D. Li, F.F. Tao, Z. Sun, Red emissive sulfur, nitrogen codoped carbon dots and their application in ion detection and theraonostics, ACS Appl. Mater. Interfaces 9 (22) (2017) 18549–18556.
- [39] J. Wan, X. Zhang, Y. Jiang, S. Xu, J. Li, M. Yu, K. Zhang, Z. Su, Regulation of multicolor fluorescence of carbonized polymer dots by multiple contributions of effective conjugate size, surface state, and molecular fluorescence, J. Mater. Chem. B 10 (36) (2022) 6991–7002.
- [40] L. Ai, Y. Yang, B. Wang, J. Chang, Z. Tang, B. Yang, S. Lu, Insights into photoluminescence mechanisms of carbon dots: advances and perspectives, Sci. Bull. 66 (8) (2021) 839–856.
- [41] H. Ding, X.-H. Li, X.-B. Chen, J.-S. Wei, X.-B. Li, H.-M. Xiong, Surface states of carbon dots and their influences on luminescence, J. Appl. Phys. 127 (23) (2020) 231101
- [42] H.-Y. Wang, L. Zhou, H.-M. Yu, X.-D. Tang, C. Xing, G. Nie, H. Akafzade, S.-Y. Wang, W. Chen, Exploration of room-temperature phosphorescence and new mechanism on carbon dots in a polyacrylamide platform and their applications for anti-counterfeiting and information encryption, Adv. Opt. Mater. 10 (15) (2022) 2200678
- [43] Y.-A. Xiong, S.-S. Duan, H.-H. Hu, J. Yao, Q. Pan, T.-T. Sha, X. Wei, H.-R. Ji, J. Wu, Y.-M. You, Enhancement of phase transition temperature through hydrogen bond modification in molecular ferroelectrics, Nat. Commun. 15 (1) (2024) 4470.
- [44] X. Miao, D. Qu, D. Yang, B. Nie, Y. Zhao, H. Fan, Z. Sun, Synthesis of carbon dots with multiple color emission by controlled graphitization and surface functionalization, Adv. Mater. 30 (1) (2018) 1704740.
- [45] J. Pola, Thermal reactive modifications of polymer surfaces by infrared laser radiation, J. Anal. Appl. Pyrol. 169 (2022) 105819.
- [46] Y. Wu, Y. Shi, H. Wang, Urea as a hydrogen bond producer for fabricating mechanically very strong hydrogels, Macromolecules 56 (12) (2023) 4491–4502.
- [47] S. Tischer, M. Börnhorst, J. Amsler, G. Schoch, O. Deutschmann, Thermodynamics and reaction mechanism of urea decomposition, PCCP 21 (30) (2019) 16785–16797.
- [48] M.M. Barbooti, D.A. Al-Sammerrai, Thermal decomposition of citric acid, Thermochim. Acta 98 (1986) 119–126.
- [49] K.E. Supan, C. Robert, M.J. Miller, J.M. Warrender, S.F. Bartolucci, Thermal degradation of MWCNT/polypropylene nanocomposites: a comparison of TGA and laser pulse heating, Polym. Degrad. Stab. 141 (2017) 41–44.